[14] J. Zhang and M. Ferch, "Rapid on-line learning of compliant motion for two-arm coordination," in *Proc. IEEE Int. Conf. Robotics and Automation*, Leuven, Belgium, May 1998, pp. 1853–1858.
[15] J. Zhang and A. Knoll, "Constructing fuzzy controllers with B-spline models," in *Proc. IEEE Int. Conf. Fuzzy Systems*, 1996, pp. 416–421.
[16] F. Caccavale, S. Chiaverini, C. Natale, B. Siciliano, and L. Villani, "Geometrically consistent impedance control for dual-robot manipulation," in *Proc. IEEE Int. Conf. Robotics and Automation*, San Francisco, CA, Apr. 2000, pp. 3874–3879.
[17] D. A. Lawrence, "Impedance control stability properties in common implementations," in *Proc. IEEE Int. Conf. Robotics and Automation*, 1988, pp. 1185–1190.
[18] H. Asada and J. J. Slotine, *Robot Analysis and Control*. New York: Wiley, 1986.
[19] H. Goldstein, *Classical Mechanics*. Reading, MA: Addison-Wesley, 1980.

A Global Output-Feedback Controller for Simultaneous Tracking and Stabilization of Unicycle-Type Mobile Robots

Khac Duc Do, Zhong-Ping Jiang, and Jie Pan

***Abstract*—We present a time-varying global output-feedback controller that solves both tracking and stabilization for unicycle-type mobile robots simultaneously at the torque level. The controller synthesis is based on a coordinate transformation, Lyapunov's direct method, and backstepping technique. Simulations demonstrate the result.**

***Index Terms*—Exponential observer, global output feedback, mobile robot, tracking and stabilization.**

I. Introduction

The main difficulty of solving stabilization and tracking control of mobile robots is due to the fact that the motion of the systems to be controlled has more degrees of freedom (DOFs) than the number of control inputs under nonholonomic constraints. Brockett's theorem [12] shows that any continuous time-invariant feedback-control law does not make the null solution of the wheeled mobile robots asymptotically stable. Over the last decade, a lot of interest has been devoted to stabilization and tracking control of nonholonomic mechanical systems, including wheeled mobile robots [1]–[9]. Tracking and stabilization are studied separately in these papers. Their objectives are mostly kinematic models. Since mobile robots do not have direct control over velocities, a static mapping implementation requires a high-gain control law and cannot achieve global results; see [19, pp. 239–245] for a discussion on general nonlinear systems. Recently, several authors focused on the dynamic model [9]–[11] using the backstepping technique [13].

To our knowledge, output-feedback tracking control of land, air, and sea vehicles has been solved for the case of fully actuated, cf. [18, pp. 311–334]. The main difficulty of designing an observer-based output feedback for Lagrange systems in general is because of the Coriolis matrix, which results in quadratic cross terms of unmeasured velocities. In addition, the nonholonomic constraints of mobile robots make the output-feedback problem more challenging. For example, many solutions proposed for robot manipulator control ([18] and references therein) cannot directly be applied. There are no currently available results on output-feedback tracking of mobile robots, although some results are proposed for a class of nonholonomic systems without any quadratic terms of unmeasured states [17]. Some recent results on output-feedback control of the single-DOF Lagrange systems were addressed in [14] (high-gain control), [15], and [16] for a nonlinear benchmark system. It is noted that the systems studied in [14]–[16] can contain a square term of only one unmeasured state. Although the author of [15] gave an extension to systems with more DOFs, but relied (see [15, Th. 5.1]) on the solution of a differential equation, which does not exist for more than one DOF, in general, and for the mobile robot in question.

Manuscript received March 18, 2003. This paper was recommended for publication by Associate Editor Z. Li and Editor A. De Luca upon evaluation of the reviewers' comments.

K. D. Do and J. Pan are with the School of Mechanical Engineering, The University of Western Australia, Crawley, WA 6009, Australia (e-mail: duc@mech.uwa.edu.au; pan@mech.uwa.edu.au).

Z.-P. Jiang is with the Department of Electrical and Computer Engineering, Polytechnic University, Brooklyn, NY 11201 USA (e-mail: zjiang@control.poly.edu).

Digital Object Identifier 10.1109/TRA.2004.825470

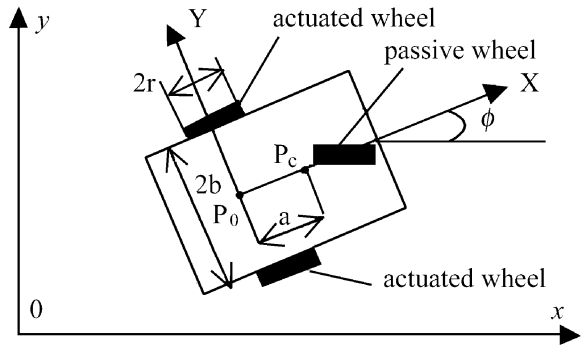

Fig. 1. Two-wheel driven mobile robot.

This paper contributes a method to design a global output-feedback controller (i.e., the controller uses only position and orientation measurements) for both stabilization and tracking of unicycle-type mobile robots at the torque level.

II. Problem Statement

We consider a two-wheel driven mobile robot (Fig. 1) whose equations of motion are given by [11]

$$\begin{aligned} \dot{\boldsymbol{\eta}} &= \mathbf{J}(\boldsymbol{\eta})\boldsymbol{\omega} \\ \mathbf{M}\dot{\boldsymbol{\omega}} + \mathbf{C}(\dot{\boldsymbol{\eta}})\boldsymbol{\omega} + \mathbf{D}\boldsymbol{\omega} &= \boldsymbol{\tau} \end{aligned} \tag{1}$$

with

$$\boldsymbol{\eta} = [x\ \ y\ \ \phi]^T, \quad \boldsymbol{\omega} = [\omega_1\ \ \omega_2]^T, \quad \boldsymbol{\tau} = [\tau_v\ \ \tau_w]^T$$

$$\mathbf{J}(\boldsymbol{\eta}) = \frac{r}{2}\begin{bmatrix} \cos(\phi) & \cos(\phi) \\ \sin(\phi) & \sin(\phi) \\ b^{-1} & -b^{-1} \end{bmatrix}, \quad \mathbf{M} = \begin{bmatrix} m_{11} & m_{12} \\ m_{12} & m_{11} \end{bmatrix}$$

$$\mathbf{D} = \begin{bmatrix} d_{11} & 0 \\ 0 & d_{22} \end{bmatrix}, \quad \mathbf{C}(\dot{\boldsymbol{\eta}}) = \begin{bmatrix} 0 & c\dot{\phi} \\ -c\dot{\phi} & 0 \end{bmatrix}$$

$$c = 0.5b^{-1}r^2 m_c a, \quad m_{11} = 0.25b^{-2}r^2(mb^2 + I) + I_w$$

$$m_{12} = 0.25b^{-2}r^2(mb^2 - I), \quad m = m_c + 2m_w$$

$$I = m_c a^2 + 2m_w b^2 + I_c + 2I_m$$

where m_c and m_w are the masses of the body and wheel with a motor; I_c, I_w, and I_m are the moment of inertia of the body about the vertical axis through P_c (center of mass), the wheel with a motor about the wheel axis, and the wheel with a motor about the wheel diameter, respectively; a, b and r are defined in Fig. 1; the positive terms $d_{ii}, i =$

1, 2 are the damping coefficients; (x, y, ϕ) are the position and orientation of the robot, ω_1 and ω_2 are the angular velocities of the wheels; and τ_v and τ_w are the control torques applied to the wheels of the robot. We assume that the reference trajectory is generated by the following virtual robot:

$$\begin{aligned} \dot{x}_d &= \cos(\phi_d)v_d \\ \dot{y}_d &= \sin(\phi_d)v_d \\ \dot{\phi}_d &= w_d \end{aligned} \tag{2}$$

where (x_d, y_d, ϕ_d) are the position and orientation of the virtual robot, and v_d and w_d are the linear and angular velocities of the virtual robot, respectively.

A. Control Objective

Under *Assumption 1*, design the control input vector $\boldsymbol{\tau}$ to force the position and orientation, (x, y, ϕ) of the real robot (1) to globally asymptotically track (x_d, y_d, ϕ_d) generated by (2) with only (x, y, ϕ) available for feedback.

Assumption 1: The reference signals v_d, $\dot{v}_d$, $\ddot{v}_d$, w_d, and $\dot{w}_d$ are bounded. In addition, one of the following conditions holds:

$$\mathbf{C1}.\ \int_0^\infty (|v_d(t)| + |w_d(t)|)\,dt \le \mu_{11} \tag{3}$$

$$\mathbf{C2}.\ \int_0^\infty |v_d(t)|\,dt \le \mu_{21} \text{ and } |w_d(t)| \ge \mu_{22} \tag{4}$$

$$\mathbf{C3}.\ \int_{t_0}^t v_d^2(\tau)d\tau \ge \mu_{31}(t-t_0) - \mu_{32}, \quad \forall t \ge t_0 \ge 0 \tag{5}$$

where μ_{11}, μ_{21}, and μ_{32} are nonnegative constants; μ_{22} and μ_{31} are strictly positive constant.

Remark 1: The problem of set-point regulation/stabilization, tracking a path approaching a set-point is included in **C1**. Tracking linear and circular paths belongs to **C3**.

Remark 2: **C2** implies that the case where the robot linear velocity is zero or approaches zero but its angular velocity is of sinusoidal type, is excluded. The reason is that our control approach is to introduce some persistent excitation (PE) signal in the robot angular velocity virtual control to handle set-point stabilization/regulation. Therefore, this case is not included, to avoid two signals canceling each other. If the reference velocity w_d is known completely in advance, the above case can be included. However, this case rarely happens in practice.

Remark 3: The problem of simultaneous stabilization and tracking not only is of theoretical interest, but also possesses some advantages over the use of separate stabilization and tracking controllers, such as only one controller and transient improvement because of no switching. Moreover, if the switching time is unknown, the separate stabilization and tracking-control approach cannot be used.

III. Observer Design

As discussed in Section I, we first remove the quadratic velocity terms in the mobile robot dynamics by introducing the following coordinate change:

$$\mathbf{X} = \mathbf{Q}(\boldsymbol{\eta})\boldsymbol{\omega} \tag{6}$$

where $\mathbf{Q}(\boldsymbol{\eta})$ is a globally invertible matrix with bounded elements to be determined. Using (6), we write the second equation of (1) as follows:

$$\dot{\mathbf{X}} = \left[\dot{\mathbf{Q}}(\boldsymbol{\eta})\boldsymbol{\omega} - \mathbf{Q}(\boldsymbol{\eta})\mathbf{M}^{-1}\mathbf{C}(\dot{\boldsymbol{\eta}})\boldsymbol{\omega}\right] + \mathbf{Q}(\boldsymbol{\eta})\mathbf{M}^{-1}(-\mathbf{D}\boldsymbol{\omega} + \boldsymbol{\tau}). \tag{7}$$

In [15], the author requires $\mathbf{Q}(\boldsymbol{\eta})$ with the above properties such that $\dot{\mathbf{Q}}(\boldsymbol{\eta}) = \mathbf{Q}(\boldsymbol{\eta})\mathbf{M}^{-1}\mathbf{C}(\dot{\boldsymbol{\eta}}), \forall \boldsymbol{\eta} \in \Re^3$, which does not exist, as a simple calculation shows.

Our method is to cancel the square bracket in the right-hand side of (7) for all $(\boldsymbol{\eta}, \boldsymbol{\omega}) \in \Re^5$. We assume that $q_{ij}(\boldsymbol{\eta})$, $i = 1, 2$, $j = 1, 2$ are the elements of $\mathbf{Q}(\boldsymbol{\eta})$. Using the first equation of (1), it is readily shown that the above square bracket is zero for all $(\boldsymbol{\eta}, \boldsymbol{\omega}) \in \Re^5$ if

$$\begin{aligned} &\frac{\partial q_{i1}}{\partial x}\cos(\phi) + \frac{\partial q_{i1}}{\partial y}\sin(\phi) + \frac{\partial q_{i1}}{\partial \phi}\frac{1}{b} + \frac{n_{12}c}{b}q_{i1} + \frac{n_{11}c}{b}q_{i2} = 0 \\ &\frac{\partial q_{i2}}{\partial x}\cos(\phi) + \frac{\partial q_{i2}}{\partial y}\sin(\phi) - \frac{\partial q_{i2}}{\partial \phi}\frac{1}{b} + \frac{n_{11}c}{b}q_{i1} + \frac{n_{12}c}{b}q_{i2} = 0 \\ &\left(\frac{\partial q_{i1}}{\partial x} + \frac{\partial q_{i2}}{\partial x}\right)\cos(\phi) + \left(\frac{\partial q_{i1}}{\partial y} + \frac{\partial q_{i2}}{\partial y}\right)\sin(\phi) \\ &\quad + \left(\frac{\partial q_{i2}}{\partial \phi} - \frac{\partial q_{i1}}{\partial \phi}\right)\frac{1}{b} - (n_{11}+n_{12})cb^{-1}(q_{i1}+q_{i2}) = 0. \end{aligned} \tag{8}$$

Using the characteristic method to solve the above partial differential equations gives a family of solutions

$$\begin{aligned} q_{i1} &= C_{i1}\sin(c\Delta\phi) + C_{i2}\cos(c\Delta\phi) \\ q_{i2} &= n_{11}^{-1}\left((C_{i2}\Delta - C_{i1}n_{12})\sin(c\Delta\phi)\right. \\ &\qquad \left. - (C_{i1}\Delta + C_{i2}n_{12})\cos(c\Delta\phi)\right) \end{aligned} \tag{9}$$

where $i = 1, 2$, $n_{11} = m_{11}(m_{11}^2 - m_{12}^2)^{-1}$, $n_{12} = -m_{12}(m_{11}^2 - m_{12}^2)^{-1}$ $\Delta = \sqrt{n_{11}^2 - n_{12}^2}$; C_{i1} and C_{i2} are arbitrary constants.

A choice of $C_{11} = C_{22} = 0$, $C_{12} = C_{21} = n_{11}$ results in

$$\mathbf{Q}(\boldsymbol{\eta}) = \begin{bmatrix} n_{11}\cos(a\Delta\phi) & \Delta\sin(a\Delta\phi) - n_{12}\cos(a\Delta\phi) \\ n_{11}\sin(a\Delta\phi) & -n_{12}\sin(a\Delta\phi) - \Delta\cos(a\Delta\phi) \end{bmatrix}. \tag{10}$$

This matrix is globally invertible and its elements are bounded. Now we write (1) in the $(\boldsymbol{\eta}, \mathbf{X})$ coordinates as

$$\begin{aligned} \dot{\boldsymbol{\eta}} &= \mathbf{J}(\boldsymbol{\eta})\mathbf{Q}^{-1}(\boldsymbol{\eta})\mathbf{X} \\ \dot{\mathbf{X}} &= -\mathbf{D}_{\boldsymbol{\eta}}(\boldsymbol{\eta})\mathbf{X} + \mathbf{Q}(\boldsymbol{\eta})\mathbf{M}^{-1}\boldsymbol{\tau} \end{aligned} \tag{11}$$

where $\mathbf{D}_{\boldsymbol{\eta}}(\boldsymbol{\eta}) = \mathbf{Q}(\boldsymbol{\eta})\mathbf{M}^{-1}\mathbf{D}\mathbf{Q}^{-1}(\boldsymbol{\eta})$. It is seen that (11) is linear in the unmeasured states. Indeed, a reduced-order observer can be designed, but it is often noise sensitive. We here use the following passive observer:

$$\begin{aligned} \dot{\hat{\boldsymbol{\eta}}} &= \mathbf{J}(\boldsymbol{\eta})\mathbf{Q}^{-1}(\boldsymbol{\eta})\hat{\mathbf{X}} + \mathbf{K_{01}}(\boldsymbol{\eta} - \hat{\boldsymbol{\eta}}) \\ \dot{\hat{\mathbf{X}}} &= -\mathbf{D}_{\boldsymbol{\eta}}(\boldsymbol{\eta})\hat{\mathbf{X}} + \mathbf{Q}(\boldsymbol{\eta})\mathbf{M}^{-1}\boldsymbol{\tau} + \mathbf{K_{02}}(\boldsymbol{\eta} - \hat{\boldsymbol{\eta}}) \end{aligned} \tag{12}$$

where $\hat{\boldsymbol{\eta}}$ and $\hat{\mathbf{X}}$ are the estimates of $\boldsymbol{\eta}$ and $\mathbf{X}$, respectively. The observer gain matrices $\mathbf{K}_{01}$ and $\mathbf{K}_{02}$ are chosen such that $\mathbf{Q_{01}} = \mathbf{K_{01}^T}\mathbf{P_{01}} + \mathbf{P_{01}}\mathbf{K_{01}}$ and $\mathbf{Q_{02}} = \mathbf{D_{\boldsymbol{\eta}}^T}(\boldsymbol{\eta})\mathbf{P_{02}} + \mathbf{P_{02}}\mathbf{D}_{\boldsymbol{\eta}}(\boldsymbol{\eta})$ are positive definite, and

$$\left(\mathbf{J}(\boldsymbol{\eta})\mathbf{Q}^{-1}(\boldsymbol{\eta})\right)^T\mathbf{P_{01}} - \mathbf{P_{02}}\mathbf{K_{02}} = 0 \tag{13}$$

with $\mathbf{P_{01}}$ and $\mathbf{P_{02}}$ being positive definite matrices. Since $\mathbf{D}_{\boldsymbol{\eta}}(\boldsymbol{\eta})$ is positive definite, $\mathbf{K_{01}}$ and $\mathbf{K_{02}}$ always exist. From (12) and (11), we have

$$\begin{aligned} \dot{\tilde{\boldsymbol{\eta}}} &= \mathbf{J}(\boldsymbol{\eta})\mathbf{Q}^{-1}(\boldsymbol{\eta})\tilde{\mathbf{X}} - \mathbf{K_{01}}\tilde{\boldsymbol{\eta}} \\ \dot{\tilde{\mathbf{X}}} &= -\mathbf{D}_{\boldsymbol{\eta}}(\boldsymbol{\eta})\tilde{\mathbf{X}} - \mathbf{K_{02}}\tilde{\boldsymbol{\eta}} \end{aligned} \tag{14}$$

where $\tilde{\boldsymbol{\eta}} = \boldsymbol{\eta} - \hat{\boldsymbol{\eta}}$ and $\tilde{\mathbf{X}} = \mathbf{X} - \hat{\mathbf{X}}$. It is now seen that (14) is globally exponentially stable by taking the Lyapunov function $V_0 = \tilde{\boldsymbol{\eta}}^T\mathbf{P_{01}}\tilde{\boldsymbol{\eta}} + \tilde{\mathbf{X}}^T\mathbf{P_{02}}\tilde{\mathbf{X}}$, whose derivative along the solution of (14) and using (13), satisfies $\dot{V}_0 = -\tilde{\boldsymbol{\eta}}^T\mathbf{Q_{01}}\tilde{\boldsymbol{\eta}} - \tilde{\mathbf{X}}^T\mathbf{Q_{02}}\tilde{\mathbf{X}}$, which, in turn, implies that there exists a strictly positive constant σ_0, such that

$$\left\|\left(\tilde{\boldsymbol{\eta}}(t), \tilde{\mathbf{X}}(t)\right)\right\| \le \left\|\left(\tilde{\boldsymbol{\eta}}(t_0), \tilde{\mathbf{X}}(t_0)\right)\right\| e^{-\sigma_0(t-t_0)}, \quad \forall t \ge t_0 \ge 0. \tag{15}$$

Define $\hat{\boldsymbol{\omega}} = [\hat{\omega}_1 \ \ \hat{\omega}_2]^T$, being an estimator of the velocity vector $\boldsymbol{\omega}$, as

$$\hat{\boldsymbol{\omega}} = \mathbf{Q}^{-1}(\boldsymbol{\eta})\hat{\mathbf{X}}. \tag{16}$$

The velocity estimate error vector, $\tilde{\boldsymbol{\omega}} = \boldsymbol{\omega} - \hat{\boldsymbol{\omega}}$ satisfies

$$\tilde{\boldsymbol{\omega}} = \mathbf{Q}^{-1}(\boldsymbol{\eta})\tilde{\mathbf{X}}. \tag{17}$$

To prepare for the control design in the next section, we convert the wheel velocities ω_1 and ω_2 to the linear, v, and angular, w, velocities of the robot by the relationship

$$[v \quad w]^T = \mathbf{B}^{-1}[\omega_1 \quad \omega_2]^T, \quad \mathbf{B} = \frac{1}{r}\begin{bmatrix} 1 & b \\ 1 & -b \end{bmatrix}. \tag{18}$$

By defining $\tilde{v} = v - \hat{v}$, $\tilde{w} = w - \hat{w}$ with $\hat{v}$ and $\hat{w}$ being estimates of v and w, we can see from (17) and (18) that

$$\|(\tilde{v}(t), \tilde{w}(t))\| \leq \gamma_0 \left\| \left(\tilde{\boldsymbol{\eta}}(t_0), \tilde{\mathbf{X}}(t_0)\right) \right\| e^{-\sigma_0(t-t_0)}, \quad \forall t \geq t_0 \geq 0 \tag{19}$$

where γ_0 is a positive constant. We now write (1) in conjunction with (16) and (18) as

$$\begin{aligned} \dot{x} &= \cos(\phi)\hat{v} + \cos(\phi)\tilde{v} \\ \dot{y} &= \sin(\phi)\hat{v} + \sin(\phi)\tilde{v} \\ \dot{\phi} &= \hat{w} + \tilde{w} \\ \dot{\hat{v}} &= \tau_{vc} + \Omega_v \\ \dot{\hat{w}} &= \tau_{wc} + \Omega_w \end{aligned} \tag{20}$$

where Ω_v and Ω_w are the first and second rows of $\mathbf{\Omega}$

$$\begin{aligned} \mathbf{\Omega} &= \mathbf{B^{-1}N_cB}\begin{bmatrix} \hat{v} \\ \hat{w} \end{bmatrix}\tilde{w} + \mathbf{B^{-1}Q^{-1}}(\boldsymbol{\eta})\mathbf{K_{02}}\tilde{\boldsymbol{\eta}} \\ \mathbf{N_c} &= c\begin{bmatrix} n_{12} & -n_{11} \\ n_{11} & -n_{12} \end{bmatrix} \end{aligned} \tag{21}$$

and we have chosen the control torque

$$\boldsymbol{\tau} = \mathbf{MB}\left(\mathbf{B^{-1}N_cB}\begin{bmatrix} \hat{v} \\ \hat{w} \end{bmatrix}\hat{w} - \mathbf{B^{-1}M^{-1}DB}\begin{bmatrix} \hat{v} \\ \hat{w} \end{bmatrix} + \begin{bmatrix} \tau_{vc} \\ \tau_{vc} \end{bmatrix}\right) \tag{22}$$

with τ_{vc} and τ_{wc} being the new control inputs to be designed in the next section.

IV. Control Design

As often done in tracking control of mobile robots [11], we first interpret the tracking errors as

$$\begin{bmatrix} x_e \\ y_e \\ \phi_e \end{bmatrix} = \begin{bmatrix} \cos(\phi) & \sin(\phi) & 0 \\ -\sin(\phi) & \cos(\phi) & 0 \\ 0 & 0 & 1 \end{bmatrix}\begin{bmatrix} x - x_d \\ y - y_d \\ \phi - \phi_d \end{bmatrix}. \tag{23}$$

Using (23), (2), and the kinematic part of (20), we have the kinematic tracking errors

$$\begin{aligned} \dot{x}_e &= \hat{v} - v_d\cos(\phi_e) + y_e(\hat{w} + \tilde{w}) + \tilde{v} \\ \dot{y}_e &= v_d\sin(\phi_e) - x_e(\hat{w} + \tilde{w}) \\ \dot{\phi}_e &= \hat{w} - w_d + \tilde{w}. \end{aligned} \tag{24}$$

Since (24) and the last two equations of (20) are of the lower triangular structure, we use the backstepping technique [13] to design τ_{vc} and τ_{wc} in two steps.

Step 1: In this step, we consider $\hat{v}$ and $\hat{w}$ as the controls. From (24), it is seen that $\hat{v}$ and $\hat{w}$ can be directly used to stabilize x_e and ϕ_e dynamics. To stabilize y_e dynamics, ϕ_e can be used when v_d is PE. When v_d is not PE (stabilization/regulation case), we need some PE signal in $\hat{w}$ to stabilize y_e dynamics via x_e. With these observations in mind, we define

$$\overline{v} = \hat{v} - \alpha_v, \quad \overline{w} = \hat{w} - \alpha_w, \quad \overline{\phi}_e = \phi_e - \alpha_{\phi e} \tag{25}$$

where α_v, α_w, and $\alpha_{\phi e}$ are the virtual controls of $\hat{v}$, $\hat{w}$, and ϕ_e, respectively. From the above discussion, we first choose the virtual controls α_v and $\alpha_{\phi e}$ as

$$\begin{aligned} \alpha_v &= -c_1\varpi_1^{-1}x_e + v_d\cos(\phi_e) \\ \alpha_{\phi e} &= -\arcsin\left(k(t)\varpi_1^{-1}y_e\right) \\ k(t) &= \lambda_1 v_d + \lambda_2\cos(\lambda_3 t) \end{aligned} \tag{26}$$

where $\varpi_1 = \sqrt{1 + x_e^2 + y_e^2}$; c_1 is a positive constant; λ_i, $i = 1, 2, 3$ are positive constants such that $|k(t)| \leq k_* < 1, \forall t$. They will be specified later. For simplification, the virtual control α_v does not cancel a known term $y_e\hat{w}$ in the x_e dynamics. It is of interest to note that the choice of (26) will result in a global result and bounded virtual velocity controls (see *Remark 4*).

To design α_w, differentiating $\overline{\phi}_e = \phi_e - \alpha_{\phi e}$ along the solution of (24), together with (26), yields

$$\begin{aligned} \dot{\overline{\phi}}_e &= \left(1 - k\varpi_2^{-1}x_e\right)(\alpha_w + \overline{w} + \tilde{w}) \\ &\quad - w_d - k\varpi_2^{-1}\varpi_1^{-2}x_e y_e(\overline{v} + \tilde{v}) \\ &\quad + \varpi_2^{-1}\left(\dot{k}y_e + kc_1\varpi_1^{-3}x_e^2 y_e + kv_d\varpi_1^{-2}\left(1 + x_e^2\right)\sin(\phi_e)\right) \end{aligned} \tag{27}$$

which suggests we choose

$$\begin{aligned} \alpha_w = \frac{1}{1 - k\varpi_2^{-1}x_e}&\left(-\frac{c_2\overline{\phi}_e}{\sqrt{1 + \phi_e^2}} + w_d - \varpi_2^{-1}\right. \\ &\left.\times\left(\dot{k}y_e + kc_1\varpi_1^{-3}x_e^2 y_e + kv_d\varpi_1^{-2}\left(1 + x_e^2\right)\sin(\phi_e)\right)\right) \end{aligned} \tag{28}$$

where $\varpi_2 = \sqrt{1 + x_e^2 + (1 - k^2)y_e^2}$; c_2 is a positive constant.

Remark 4: From (26) and (28), the virtual controls α_v and α_w, as a simple calculation shows, are bounded by some constants depending on the upper bound of v_d, $\dot{v}_d$, and w_d.

Substituting (26) and (28) into (24) and (27) results in

$$\begin{aligned} \dot{x}_e &= -c_1\varpi_1^{-1}x_e + y_e(\hat{w} + \tilde{w}) + \overline{v} + \tilde{v} \\ \dot{y}_e &= -k\varpi_1^{-1}v_d y_e - x_e(\hat{w} + \tilde{w}) \\ &\quad + v_d\varpi_1^{-1}\left(\sin(\overline{\phi}_e)\varpi_2 - \left(\cos(\overline{\phi}_e) - 1\right)ky_e\right) \\ \dot{\overline{\phi}}_e &= -\frac{c_2\overline{\phi}_e}{\sqrt{1 + \phi_e^2}} + \left(1 - k\varpi_2^{-1}x_e\right)(\overline{w} + \tilde{w}) \\ &\quad - k\varpi_2^{-1}\varpi_1^{-2}x_e y_e(\overline{v} + \tilde{v}). \end{aligned} \tag{29}$$

Step 2: At this step, the control inputs τ_{vc} and τ_{wc} are designed. We note that α_v is a smooth function of x_e, y_e, ϕ_e, and v_d, and that α_w is a smooth function of x_e, y_e, ϕ_e, v_d, $\dot{v}_d$, w_d, and t.

By differentiating $\overline{v} = \hat{v} - \alpha_v$ and $\overline{w} = \hat{w} - \alpha_w$ along the solution of (24) and the last two equations of (20), and noting the last equation of (29), we choose τ_{vc} and τ_{wc} as

$$\begin{aligned} \tau_{vc} &= -c_3\overline{v} + \frac{\partial\alpha_v}{\partial x_e}\left(\hat{v} - v_d\cos(\phi_e) + y_e\hat{w}\right) \\ &\quad + \frac{\partial\alpha_v}{\partial\phi_e}(\hat{w} - w_d) + \frac{\partial\alpha_v}{\partial y_e}\left(v_d\sin(\phi_e) - x_e\hat{w}\right) \\ &\quad + \frac{\partial\alpha_v}{\partial v_d}\dot{v}_d - \delta_v(\hat{v}^2 + \hat{w}^2)\overline{v} + k\varpi_2^{-1}\varpi_1^{-2}x_e y_e\overline{\phi}_e \\ \tau_{wc} &= -c_4\overline{w} + \frac{\partial\alpha_w}{\partial x_e}\left(\hat{v} - v_d\cos(\phi_e) + y_e\hat{w}\right) \\ &\quad + \frac{\partial\alpha_w}{\partial\phi_e}(\hat{w} - w_d) + \frac{\partial\alpha_w}{\partial y_e}\left(v_d\sin(\phi_e) - x_e\hat{w}\right) \\ &\quad + \frac{\partial\alpha_w}{\partial v_d}\dot{v}_d\frac{\partial\alpha_w}{\partial\dot{v}_d}\ddot{v}_d + \frac{\partial\alpha_w}{\partial w_d}\dot{w}_d - \left(1 - k\varpi_2^{-1}x_e\right)\overline{\phi}_e \\ &\quad - \delta_w(\hat{v}^2 + \hat{w}^2)\overline{w} \end{aligned} \tag{30}$$

where c_3, c_4, δ_v, and δ_w are positive constants. The terms multiplied by δ_v and δ_w are the nonlinear damping terms to overcome the effect of observer errors, see (21). The choice of (30) results in

$$\begin{aligned}\dot{\overline{v}} =& -c_3\overline{v} - \frac{\partial\alpha_v}{\partial x_e}(y_e\tilde{w}+\tilde{v}) - \frac{\partial\alpha_v}{\partial\phi_e}\tilde{w} + \frac{\partial\alpha_v}{\partial y_e}x_e\tilde{w}\\ &+\Omega_v - \delta_v(\hat{v}^2+\hat{w}^2)\overline{v} + k\varpi_2^{-1}\varpi_1^{-2}x_e y_e\overline{\phi}\\ \dot{\overline{w}} =& -c_4\overline{w} - \frac{\partial\alpha_w}{\partial x_e}(y_e\tilde{w}+\tilde{v}) - \frac{\partial\alpha_w}{\partial\phi_e}\tilde{w} + \frac{\partial\alpha_w}{\partial y_e}x_e\tilde{w}\\ &+\Omega_w - \left(1-k\varpi_2^{-1}x_e\right)\overline{\phi}_e - \delta_w(\hat{v}^2+\hat{w}^2)\overline{w}. \end{aligned} \tag{31}$$

To analyze the closed loop consisting of (29) and (31), we first consider the $(\overline{\phi}_e, \overline{v}, \overline{w})$ subsystem, then move to the (x_e, y_e) subsystem.

A. $(\overline{\phi}_e, \overline{v}, \overline{w})$ *Subsystem*

For this subsystem, consider the Lyapunov function

$$V_1 = 0.5\left(\overline{\phi}_e^2 + \overline{v}^2 + \overline{w}^2\right) \tag{32}$$

whose derivative along the solution of the last equation of (29) and (31) satisfies

$$\begin{aligned}\dot{V}_1 \le& -\frac{c_2\overline{\phi}_e^2}{\sqrt{1+\overline{\phi}_e^2}} - c_3\overline{v}^2 - c_4\overline{w}^2 + (\chi_{11}+\chi_{12}V_1)e^{-\sigma_0(t-t_0)}\\ \le& (\chi_{11}V_1+\chi_{12})e^{-\sigma_0(t-t_0)}\end{aligned} \tag{33}$$

where χ_{11} and χ_{12} are class-K functions of $\|(\tilde{\boldsymbol{\eta}}(t_0), \tilde{\mathbf{X}}(t_0))\|$. The second line of (33) implies that $V_1(t) \le \chi_{13}$, with χ_{13} being a class-K function of $\|(\tilde{\boldsymbol{\eta}}(t_0), \tilde{\mathbf{X}}(t_0), \overline{\mathbf{X}}(t_0))\|$ and $\overline{\mathbf{X}}(t) = |\overline{\phi}_e(t)\overline{v}(t)\overline{w}(t)|^T$. Substituting this bound into the first line of (33) yields

$$\dot{V}_1 \le -2\min\left(\frac{c_2}{\sqrt{1+2\chi_{13}}}, c_3, c_4\right)V_1 + (\chi_{11}+\chi_{12}\chi_{13})e^{-\sigma_0(t-t_0)} \tag{34}$$

which implies that there exist $\sigma_1 > 0$ and a class-K function χ_1 depending on $\|(\tilde{\boldsymbol{\eta}}(t_0), \tilde{\mathbf{X}}(t_0), \overline{\mathbf{X}}(t_0))\|$ such that $\|\overline{\mathbf{X}}(t)\| \le \chi_1 e^{-\sigma_1(t-t_0)}$, i.e., the $(\overline{\phi}_e, \overline{v}, \overline{w})$ subsystem is globally asymptotically stable.

B. (x_e, y_e) *Subsystem*

We first prove that the trajectories (x_e, y_e) are bounded by taking the Lyapunov function

$$V_2 = \sqrt{1+x_e^2+y_e^2} - 1 \tag{35}$$

whose derivative along the solution of the first two equations of (29) satisfies

$$\begin{aligned}\dot{V}_2 \le& -c_1\varpi_1^{-2}x_e^2 - kv_d\varpi_1^{-2}y_e^2 + \chi_{21}e^{-\sigma_{21}(t-t_0)}\\ \le& \lambda_2 v_d\cos(\lambda_3 t)\varpi_1^{-2}y_e^2 + \chi_{21}e^{-\sigma_{21}(t-t_0)}\end{aligned} \tag{36}$$

where $\sigma_{21} = \min(\sigma_0, \sigma_1)$ and χ_{21} is a class-K function of $\|(\tilde{\boldsymbol{\eta}}(t_0), \tilde{\mathbf{X}}(t_0), \overline{\mathbf{X}}(t_0))\|$. Integrating both sides of the second line of (36) yields

$$V_2(t) \le V_2(t_0) + 2\lambda_2 v_d^{\max} + \frac{\chi_{21}}{\sigma_{21}} \le \chi_{22} \tag{37}$$

where $v_d^{\max}$ is the upper bound of $|v_d(t)|$. Therefore, the trajectories (x_e, y_e) are bounded on $[0, \infty)$. To prove convergence of (x_e, y_e) to zero, we consider each case of *Assumption 1*.

Cases ***C1*** *and* ***C2****:* From the first line of (36) and noting (26), we have

$$\dot{V}_2 \le -C_1\varpi_1^{-2}x_e^2 + |\lambda_2 v_d| + \chi_{21}(\bullet)e^{-\sigma_{21}(t-t_0)}. \tag{38}$$

By integrating both sides of (38) and Barbalat's lemma in [13], we have $\lim_{t\to\infty} x_e(t) = 0$. To prove that $\lim_{t\to\infty} y_e(t) = 0$, applying [9, Lemma 2] to the first equation of (29) yields

$$\lim_{t\to\infty}\left(y_e(\alpha_w + \overline{w} + \tilde{w}) + \tilde{v} + \overline{v}\right) = 0 \tag{39}$$

which is equivalent to

$$\lim_{t\to\infty}\Xi(t) = 0 \tag{40}$$

where

$$\Xi(t) = y_e(t)\left(\frac{\dot{k}(t)y_e(t)}{\sqrt{1+(1-k^2(t))\,y_e^2(t)}} - w_d(t)\right). \tag{41}$$

On the other hand, from (38), we have

$$\frac{d}{dt}\left(V_2 - \int_0^t |\lambda_2 v_d(\tau)|\,d\tau + \sigma_{21}^{-1}\chi_{21}(\bullet)e^{-\sigma_{21}(t-t_0)}\right) \le 0 \tag{42}$$

which means that $V_2 - \int_0^t |\lambda_2 v_d(\tau)|d\tau + \sigma_{21}^{-1}\chi_{21}(\bullet)e^{-\sigma_{21}(t-t_0)}$ is nonincreasing. Since V_2 is bounded from below by zero, V_2 tends to a finite nonnegative constant, depending on $\|\overline{\mathbf{X}}_e(t_0)\|$ with $\overline{\mathbf{X}}_e = (x_e, y_e, \overline{\mathbf{X}}, \tilde{\boldsymbol{\eta}}(t_0), \hat{\mathbf{X}}(t_0))$. This implies that the limit of $|y_e(t)|$ exists and is finite, say l_{y_e}. If l_{y_e} was not zero, there would exist a sequence of increasing time instants $\{t_i\}_{i=1}^{\infty}$ with $t_i \to \infty$, such that both of the limits of $\dot{k}(t_i)$ and $\Xi(t_i)$ are not zero. With this in mind, if we choose $\lambda_i \ne 0$ such that

$$\frac{\lambda_2\lambda_3}{\sqrt{1-k_*^2}} < \mu_{22} \tag{43}$$

then under conditions (3) and (4), $\dot{k}(t_i)$ and $\Xi(t_i)$ cannot be nonzero simultaneously for any t_i. Hence, l_{y_e} must be zero, which allows us to conclude from (40) that $\lim_{t\to\infty} y_e(t) = 0$, i.e., the (x_e, y_e) subsystem is asymptotically stable.

Case ***C3****:* In this case, from (36), we have

$$\dot{V}_2 \le -\varpi_1^{-2}\left(c_1x_e^2 + \left(\lambda_1 v_d^2 - \lambda_2|v_d|\right)y_e^2\right) + \chi_{21}e^{-\sigma_{21}(t-t_0)} \tag{44}$$

which means that there exist $\sigma_2 > 0$ and a class-K function χ_2, depending on $\|\overline{\mathbf{X}}(t_0)\|$ such that

$$\|(x_e(t), y_e(t))\| \le \chi_2\sigma^{-\sigma_2(t-t_0)} \tag{45}$$

as long as

$$\lambda_1\mu_{31} - \lambda_2 v_d^{\max} \ge \mu_{31}^* \tag{46}$$

where μ_{31}^* is a positive constant. In addition, it can be shown that in this case, the closed loop of (29) and (31) is also locally exponential stable. Under *Assumption 1*, there always exist λ_i such that (43) and (46). We have thus proven the following result.

Theorem 1: Under *Assumption 1*, the output-feedback control laws consisting of (22) and (30) force the mobile robot (1) to globally asymptotically track the virtual vehicle (2) if the constants λ_i, $i = 1, 2, 3$ are chosen such that $\lambda_i \ne 0$, (43), and (46) hold.

V. Simulations

The physical parameters are taken from [11] $r = 0.15$, $b = 0.75$, $a = 0.3$, $m_c = 30$, $m_w = 1$, $I_c = 15.625$, $I_w = 0.005$, $I_m = 0.0025$, and $d_{11} = d_{22} = 10$. We perform two simulations. For the first simulation, the reference velocities are chosen as $v_d = 0.5(\tanh(t_s - t) + 1)$, $w_d = 0$, where t_s is a positive constant. A switching combination of a tracking controller and a stabilization one in the literature cannot be used to fulfill this task if t_s is unknown in advance. A calculation shows that for $t \le t_s$ (tracking a curve), condition **C3** holds with $\mu_{31} = 0.25$, and for $t > t_s$, (parking) **C1** holds. Hence, our proposed controller can be applied. We also assume that due to some sudden impact at the time $t_m > t_s$, the robot position is perturbed to

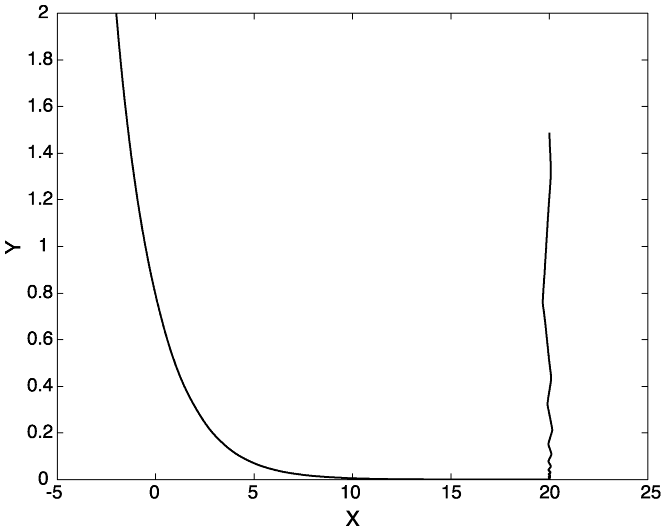

Fig. 2. First simulation: Robot position in (x,y) plane.

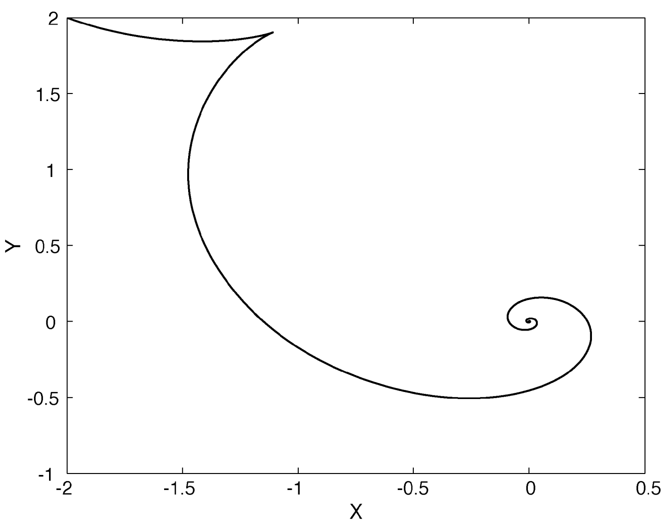

Fig. 3. Second simulation: Robot position in (x,y) plane.

$y = y_m \neq 0$ to illustrate the regulation ability of our proposed controller. For the second simulation, the reference velocities are $v_d = 0$, $w_d = 0.2$, i.e., **C2** holds with $\mu_{22} = 0.2$. The initial conditions are

$$(\boldsymbol{\eta}^{\mathbf{T}}, \boldsymbol{\omega}^{\mathbf{T}}) = ((-2, 2, -0.5), (0, 0))$$
$$(\hat{\boldsymbol{\eta}}^{\mathbf{T}}, \hat{\mathbf{X}}^{\mathbf{T}}) = ((0, 0, 0), (0, 0))$$
$$(x_d, y_d, \phi_d) = (0, 0, 0)$$

and we take $t_s = 20$, $t_m = 30$, and $y_m = 1.5$.

The control and observer gains are chosen as

$$c_i = 2, \quad 1 \leq i \leq 4, \quad \delta_v = \delta_w = 0.1$$
$$\mathbf{P_{01}} = \mathbf{P_{02}} = \mathrm{diag}(1, 1), \quad \lambda_1 = \lambda_3 = 0.5, \quad \lambda_2 = 0.1$$
$$\mathbf{K_{01}} = \mathrm{diag}(1, 1), \quad \mathbf{K_{02}} = \left(\mathbf{J}(\boldsymbol{\eta})\mathbf{Q}^{-1}(\boldsymbol{\eta})\right)^{\mathbf{T}}.$$

The above choice satisfies requirements in *Theorem 1*. Results are plotted in Figs. 2 and 3 (robot position in (x,y) plane). The tracking errors in the form of $\sqrt{x_e^2 + y_e^2 + \phi_e^2}$ are plotted in Fig. 4. Fig. 4 indicates that convergence of the tracking errors for the case of regulation to zero is much slower than for the other cases, which is a quite well-known effect when using the smooth time-varying controllers. Convergence of tracking errors in the case of **C2** is slower than that in the case of **C3**, since **C3** yields local exponential stability but only asymptotic for **C2** (see proof of *Theorem 1*).

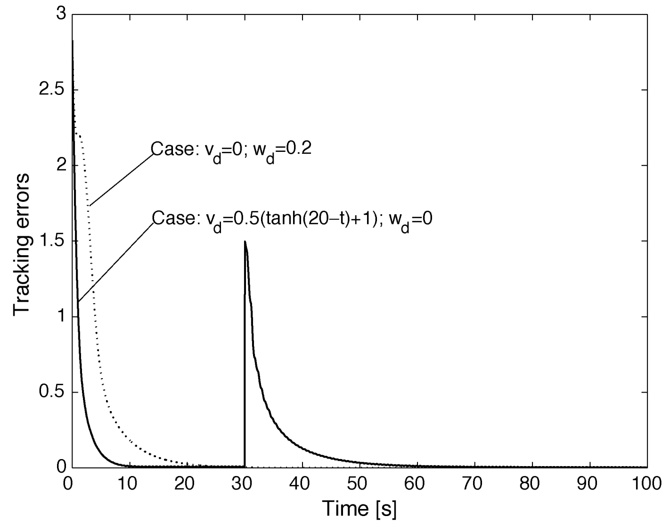

Fig. 4. Tracking errors with respect to the first and second simulations.

VI. Conclusions

A global output-feedback controller has been presented to solve both tracking and stabilization for unicycle-type mobile robots simultaneously at the torque level. The keys to success of our proposed control design are the coordinate transformation (6) and $\alpha_{\phi e}$ in (26). Future work is to extend the proposed method to a class of mechanical systems. Indeed, the main difficulty is to solve the partial differential equations similar to (8) to obtain a suitable coordinate transformation.

References

[1] A. Astolfi, “Discontinuous control of nonholonomic systems,” *Syst. Contr. Lett.*, vol. 27, pp. 37–45, 1996.

[2] A. Behal, D. M. Dawson, W. E. Dixon, and Y. Fang, “Robust tracking and regulation control for mobile robots,” in *Proc. IEEE Conf. Control and Applications*, 1999, pp. 2150–2155.

[3] C. Canudas de Wit, B. Siciliano, and G. Bastin, Eds., *Theory of Robot Control*. London, U.K.: Springer-Verlag, 1996.

[4] C. Samson and K. Ait-Abderahim, “Feedback control of a nonholonomic wheeled cart in Cartesian space,” in *Proc. IEEE Int. Conf. Robotics and Automation*, 1991, pp. 1254–1259.

[5] C. Samson, “Control of chained systems application to path following and time-varying point stabilization of mobile robots,” *IEEE Trans. Automat. Contr.*, vol. 40, pp. 64–77, Jan. 1995.

[6] I. Kolmanovsky and N. H. McClamroch, “Developments in nonholonomic control problems,” *IEEE Contr. Syst. Mag.*, vol. 15, pp. 20–36, June 1995.

[7] J.-M. Yang and J.-H. Kim, “Sliding mode control for trajectory tracking of nonholonomic wheeled mobile robots,” *IEEE Trans. Robot. Automat.*, vol. 15, pp. 578–587, June 1999.

[8] T. C. Lee, K. T. Song, C. H. Lee, and C. C. Teng, “Tracking control of unicycle-modeled mobile robots using a saturation feedback controller,” *IEEE Trans. Contr. Syst. Technol.*, vol. 9, pp. 305–318, Feb. 2001.

[9] Z. P. Jiang and H. Nijmeijer, “Tracking control of mobile robots: A case study in backstepping,” *Automatica*, vol. 33, pp. 1393–1399, 1997.

[10] R. Fierro and F. L. Lewis, “Control of a nonholonomic mobile robot: Backstepping kinematics into dynamics,” in *Proc. IEEE/RSJ Int. Workshop Intelligent Robots and Systems*, 1991, pp. 193–198.

[11] T. Kukao, H. Nakagawa, and N. Adachi, “Adaptive tracking control of nonholonomic mobile robot,” *IEEE Trans. Robot. Automat.*, vol. 16, pp. 609–615, Oct. 2000.

[12] R. W. Brockett, “Asymptotic stability and feedback stabilization,” in *Differential Geometric Control Theory*, R. W. Brockett, R. S. Millman, and H. J. Sussmann, Eds. New York: Springer-Verlag, 1983, pp. 181–191.

[13] M. Krstic, I. Kanellakopoulos, and P. V. Kokotovic, *Nonlinear and Adaptive Control Design*. New York: Wiley, 1995.

[14] A. Loria, "Global tracking control of one-degree-of-freedom Euler–Lagrange systems without velocity measurement," *Eur. J. Contr.*, pp. 144–151, 1996.

[15] G. Besancon, "Global output feedback tracking control for a class of Lagrangian systems," *Automatica*, vol. 36, pp. 1915–1921, 2000.

[16] Z. P. Jiang and I. Kanellakopoulos, "Global output-feedback tracking for a benchmark nonlinear system," *IEEE Trans. Automat. Contr.*, vol. 45, pp. 1023–1027, May 2000.

[17] Z. P. Jiang, "Lyapunov design of global state and output feedback trackers for nonholonomic control systems," *Int. J. Contr.*, vol. 73, no. 9, pp. 744–761, 2000.

[18] H. Nijmeijer and T. I. Fossen, Eds., *New Directions in Nonlinear Observer Design*. London, U.K.: Springer-Verlag, 1999.

[19] R. Sepulchre, M. Jankovic, and P. Kokotovic, *Constructive Nonlinear Control*. New York: Springer-Verlag, 1997.

Adaptive Tracking Control of Underwater Vehicle-Manipulator Systems Based on the Virtual Decomposition Approach

Gianluca Antonelli, Fabrizio Caccavale, and Stefano Chiaverini

***Abstract*—A novel adaptive control law for the end-effector tracking problem of underwater vehicle-manipulator systems (UVMSs) is presented in this paper. By exploiting the serial-chain kinematic structure of the UVMS, the overall control problem is decomposed in a set of elementary control problems, each of them formulated with respect to a single rigid body in the system. The proposed approach results in a modular control scheme which simplifies application to UVMSs with a large number of links, reduces the required computational burden, and allows efficient implementation on distributed computing architectures. Furthermore, the occurrence of kinematic and representation singularities is overcome, respectively, by expressing the control law in body-fixed coordinates and representing the attitude via the unit quaternion. To show the effectiveness of the proposed control strategy, a simulation case study is developed for a vehicle in spatial motion carrying a six-degree-of-freedom manipulator.**

***Index Terms*—Adaptive control, control of redundant manipulators, underwater robotics, virtual decomposition control.**

I. Introduction

The use of autonomous underwater vehicles (AUVs) equipped with an underwater vehicle-manipulator system (UVMS) to perform complex underwater tasks gives rise to challenging control problems involving nonlinear, coupled, and high-dimensional systems. Currently, the state of the art is represented by teleoperated master/slave architectures; few research centers are equipped with autonomous systems [26].

Several control strategies based on perfect compensation of the UVMS's dynamics have been proposed [6], [18]. However, it must be pointed out that exact knowledge of the system dynamics rarely can be assumed, especially for underwater applications, where some dynamic terms strongly depend on the environmental conditions (e.g., hydrodynamic forces).

To overcome this problem, adaptive control laws have been proposed, e.g., [13] and [14]. These approaches regard the UVMS model as a whole, thus giving rise to high-dimensional problems. In fact, differently from the case of earth-fixed manipulators, in the case of UVMS, it is not possible to reduce the number of dynamic parameters to be adapted, since the base of the manipulator (i.e., the vehicle) has full mobility. In detail, it can be stated that the computational load of such control algorithms grows as much as the fourth-order power of the number of the system's degrees of freedom (DOFs). For this reason, practical application of adaptive control to UVMS has been usually limited, even in simulation, to vehicles carrying arms with very few joints (i.e., two or three) and usually performing planar tasks.

An interesting approach is proposed in [10], where an adaptive control law, based on the micro–macro manipulator concept, is designed for UVMSs carrying a nonredundant manipulator (e.g., with 6 DOFs). The approach needs the computation of the inverse kinematics (IK) of the system; this is achieved by using the inverse of the Jacobian matrix. Hence, the approach can be applied only to nonredundant manipulators (i.e., characterized by a square Jacobian matrix) in nonsingular configurations (i.e., full-rank Jacobian matrix).

As for nonadaptive approaches, in [9] the dynamic coupling between vehicle and manipulator is investigated. From the analysis of a specific UVMS structure, a sliding-mode approach, based on the approach in [24], with a feedforward compensation term is proposed. Numerical simulation results show that the knowledge of the dynamics allows improvement of the tracking performance. This approach, however, requires knowledge of the symbolic expression for the interaction between the first link and the vehicle.

Reference [15] reports a control algorithm in which the importance of the compensation of the vehicle/manipulator interaction is highlighted by the use of a force/torque sensor on the manipulator base or, in alternative, by the use of a disturbance observer. An adaptive, non-regressor-based control law for UVMSs is also presented in [27].

In sum, adaptive model-based control approaches for UVMSs are often based on the Lagrange formulation of the dynamic model of the whole system. This leads to computationally intensive control algorithms. On the other hand, nonadaptive approaches typically require accurate knowledge of the dynamic model of the system or have to be designed for specific UVMSs. This drawback strongly limits the application of model-based control for underwater applications. Hence, in practice, control engineers adopt simple control laws (e.g., of the proportional-integral-derivative (PID) type), which usually provide significantly limited tracking performance of the control system in the face of a light computational effort.

This paper is aimed at developing a new adaptive control scheme for the tracking problem of UVMS, which keeps the advantages of model-based adaptive control, in terms of tracking accuracy, while limiting the computational load. Also, the control algorithm is designed so as to have a modular structure. This brings several advantages in terms of control software design and maintenance.

The control scheme is based on the virtual decomposition approach in [28]. Different from previous approaches, the serial-chain structure of the UVMS is exploited to decompose the overall motion-control problem in a set of elementary control problems regarding the motion of each rigid body in the system, namely, the manipulator's links and the vehicle. For each body, a control action is designed to assign the desired motion, to adaptively compensate for the body dynamics, and

Manuscript received January 14, 2003; revised April 23, 2003. This paper was recommended for publication by Associate Editor J. Leonard and Editor I. Walker upon evaluation of the reviewers' comments.

G. Antonelli and S. Chiaverini are with the Dipartimento di Automazione, Elettromagnetismo, Ingegneria dell'Informazione e Matematica Industriale, Università degli Studi di Cassino, 03043 Cassino, Italy (e-mail: antonelli@unicas.it; chiaverini@unicas.it).

F. Caccavale is with the Dipartimento di Ingegneria e Fisica dell'Ambiente, Universià degli Studi della Basilicata, 85100 Potenza, Italy (e-mail: caccavale@unibas.it).

Digital Object Identifier 10.1109/TRA.2004.825521